Available online at www.sciencedirect.com
SCIENCE DIRECT®
Journal of Theoretical Biology 239 (2006) 334–350
Journal of Theoretical Biology
www.elsevier.com/locate/yjtbi

A cellular automata model of tumor–immune system interactions

D.G. Mallet[a,b,*], L.G. De Pillis[b]

[a]School of Mathematical Sciences, Queensland University of Technology, GPO Box 2434, Brisbane, QLD 4001, Australia
[b]Center for Quantitative Life Sciences and Department of Mathematics, Harvey Mudd College, 301 East Twelfth Street, Claremont, CA 91711, USA

Received 24 November 2004; received in revised form 21 July 2005; accepted 1 August 2005
Available online 15 September 2005

Abstract

We present a hybrid cellular automata–partial differential equation model of moderate complexity to describe the interactions between a growing tumor next to a nutrient source and the immune system of the host organism. The model allows both temporal and two-dimensional spatial evolution of the system under investigation and is comprised of biological cell metabolism rules derived from both the experimental and mathematical modeling literature. We present numerical simulations that display behaviors which are qualitatively similar to those exhibited in tumor–immune system interaction experiments. These include spherical tumor growth, stable and unstable oscillatory tumor growth, satellitosis and tumor infiltration by immune cells. Finally, the relationship between these different growth regimes and key system parameters is discussed.

Keywords: Tumor; Immune; Cellular automata; Lymphocyte infiltration; Oscillatory growth

1. Introduction

The response of the immune system to mutated and potentially cancerous cells is the body's natural defense against tumor growth. Both the functioning of the immune system and the growth of tumors involve highly complex processes, and coupled, the tumor–immune interactions form an elaborate system that is not yet fully understood by either experimentalists or theoreticians.

Tumor growth and the dynamics of the immune system have been a significant focus for mathematical modeling over the past three decades. Evolving from the early chemical diffusion and differential equation models of Burton (1966) and Greenspan (1972), descriptions of tumor growth have been presented more recently using partial differential equations (PDEs) (see for example Byrne and Chaplain, 1996, 1997; Owen and Sherratt, 1997; Mallet, 2004; Pettet et al., 2001) and cellular automata (CA) (see for example Alarcon et al., 2003; Dormann and Deutsch, 2002; Bard Ermentrout and Edelstein-Keshet, 1993; Ferreira et al., 2002; Kansal et al., 2000; Patel et al., 2001). An excellent review of mathematical models of tumor growth was recently given by Araujo and McElwain (2004).

Similarly, a variety of mathematical models exist describing the immune system in its various roles. Perelson provides a substantial review of the immune system before demonstrating the process of modeling the immune system from the point of view of a physicist (Perelson and Weisbuch, 1997). Seiden and Celada (1992) developed a computer program based on a bit-string cellular automata called the IMMSIM model. The IMMSIM model in its current form includes both the humoral and cellular immune responses. A number of researchers have also modeled the kinetics of the cellular immune response, including Merrill (1982), Callewaert et al. (1988), and Perelson and Mackean (1984).

A number of mathematical models also have coupled tumor growth with immune system dynamics. Usually, these models are fully deterministic, comprised of a

*Corresponding author. School of Mathematical Sciences, Queensland University of Technology, GPO Box 2434, Brisbane, QLD 4001, Australia. Tel.: +617 3864 2354; fax: +617 3864 2310.
E-mail address: dg.mallet@qut.edu.au (D.G. Mallet).

0022-5193/$ - see front matter © 2005 Elsevier Ltd. All rights reserved.
doi:10.1016/j.jtbi.2005.08.002

series of ordinary or partial differential equations (ODEs or PDEs) describing the dynamics of, for example, tumor cells, host cells, and immune cells (Arciero et al., 2004; Bellomo et al., 1999; Bellomo and Preziosi, 2000; Galach, 2003; Kirschner and Panetta, 1998; Kuznetsov and Knott, 2001; Lin, 2004; Matzavinos and Chaplain, 2004; Owen and Sherratt, 1997, 1998; Owen et al., 2004; de Pillis and Radunskaya, 2003a; Takayanagi and Ohuchi, 2001). An excellent review of tumor–immune system models, both at the cellular and sub-cellular levels, is given by Adam and Bellomo (1997). Immunotherapy has also been investigated using similar deterministic models coupled with optimal control theory (Burden et al., 2004; de Pillis and Radunskaya, 2001, 2003b).

Most of these tumor–immune system models are fully deterministic, and although there are several excellent models that include spatial interactions between tumor and immune cells using chemotaxis terms in the governing PDEs, simulation results often focus mainly on one-dimensional or radially symmetric spatial growth and the temporal evolution of the cell species under investigation (Matzavinos and Chaplain, 2004; Owen and Sherratt, 1997; Owen et al., 2004). In this paper, we also model temporal evolutions but furthermore include two-dimensional spatial evolution by employing a hybrid cellular automata–partial differential equation modeling approach.

This deterministic–stochastic approach has the benefits of being conceptually accessible and computationally straightforward to implement. Unlike the spatio-temporal models noted above, this model allows for the consideration of individual cell behavior and associated randomness, rather than applying a general rule to a collection of cells (for example, with regard to cell migration). Because of the structure of the model, which simulates chemical diffusion through deterministic PDEs and cell behavior through a set probabilistic rules, the model and its computational implementation are very flexible. It can easily be extended or modified as new data become available or when different situations arise requiring the inclusion of new chemical species or cell behavior rules.

Few if any other models, consider the spatio-temporal and partially stochastic interactions between individual tumor cells and multiple populations of individually recognised immune cells, such as is the case in this work. Furthermore, biologists and immunologists also have a limited understanding of such interactions. As such we believe it is important to focus on early tumor growth before tackling the more complicated vascularised stages of growth in such an investigation.

It should also be noted that the strategy employed in this work to describe the tumor dynamics and interactions with the immune system is quite different from the continuous–discrete hybrid used by Anderson and Chaplain (1998) in their models of angiogenesis. Anderson and Chaplain employ discrete models closely related to continuous PDE-based angiogenesis models whereas in this work we consider a mixture of continuous PDEs for chemical quantities and a discrete cell-based description for biological cell species with phenomenologically sourced probabilities for cell dynamics. It is also different from the off-lattice approach, another technique that can be used in this type of research, which is employed by Drasdo and coworkers (Drasdo and Loeffler, 2001; Galle et al., 2005) and allows for the modeling of forces on the cells (such as deformation forces).

The hybrid CA–PDE modeling approach has been successfully used in the past to model tumor growth, chemotherapeutic treatment and the effects of vascularization on tumor growth (Patel et al., 2001; Ferreira et al., 2002; Alarcon et al., 2003; Ferreira et al., 2003). Here we use reaction–diffusion PDEs to describe chemical species such as growth nutrients, and a cellular automata strategy to track the tumor as well as two distinct immune cell species. Together, these elements simulate the growth of the tumor and the interactions of the immune cells with the tumor–growth.

Using the hybrid CA–PDE model, we aim to demonstrate the combined effects of the innate and specific immune systems on the growth of a two-dimensional tumor. This is accomplished through the development of a model with cellular behaviors related to those described in the experimental literature and by considering the ODE models of tumor–immune system interactions developed in other works (such as Kuznetsov and Knott, 2001; de Pillis and Radunskaya, 2001, 2003b).

This model is useful because it allows for predictions to be made with regard to the behavior of the initial stages of solid tumor growth and the growth of undetectable metastases. In this model, we study a cluster of tumor cells to which nutrient is made available through a nearby blood vessel. Note that in a model of later stage development, one might wish to incorporate nutrient delivery through blood vessel sources interspersed throughout the tumor cell cluster as has been attempted by Alarcon et al. (2003), McDougal et al. (2002) and Gatenby and Gawlinski (1996). However, in this work we focus on the early stage model as the study of early stage tumor models continues to be of interest (see, for example, Owen and Sherratt, 1998, 1999; Smallbone et al., 2005; Byrne and Chaplain, 1995; Byrne, 1997; Please et al., 1999; Ward and King, 1997, 1999; Franks et al., 2003, 2003, 2005; Owen et al., 2004; Preziosi, 2003; Xu, 2004). One of the reasons for modeling tumor growth in its early stages is to allow for the development and validation of a foundational model prior to the inclusion of potentially confounding model features such as full vascularization and

metastatic behavior. Another reason is to allow for the modeling of the situation in which a patient whose primary tumor has been resected, but who may additionally require post-operative therapy to ensure that undetectable metastases are being treated. These undetectable metastases are reasonably modeled as early stage tumors.

We will demonstrate different types of tumor growth including spherical and papillary (branchy) growth, stable and unstable oscillatory growth, and lymphocyte-infiltrated growth, and show the dependence of these different morphologies on key model parameters related to the tumor–immune system interactions. The model developed here is also useful as it provides an extension to previous models lacking an immune system component, that may be built upon in the future with the addition of other cell and chemical species in order to test and validate new hypotheses.

In a study of cell transfer therapy for metastatic melanoma patients, Rosenberg et al. (2003) comment on the difficulty of deriving meaningful results from human experiments due to the variations in cell types, tumor types, immune states, and more fundamentally the human subjects themselves. While Rosenberg et al. suggest a solution to such a problem is to treat the same patient in differing ways over a period of time, another more flexible and less hazardous method is through mathematical modeling—the pathway taken in this paper to examine the effects of the immune system on tumors.

In Section 2 we present a short overview of the biology underlying the mathematical model that will be developed in Section 3. In Section 4, a number of representative simulation outputs are presented along with a discussion of the model results in general. Finally, in Section 5, the results of the model simulations are discussed and related to the biological problem, and a number of ideas for future research are proposed.

2. Biological background

Consider first the biology underlying the growth of a tumor. In normal tissue, division and death of cells are tightly balanced. This balance allows the body to construct and maintain the tissue so that it may carry out its particular purpose in the survival of the organism. The growth of a tumor starts with a single mutated cell that is able to proliferate inappropriately by either avoiding apoptosis or undergoing excessive proliferation. This leads to an imbalance in the cell death:division ratio when compared with that observed in normal tissue (Kleinsmith et al., 2001; Weinberg, 1996).

In this paper we consider a tumor in the early stage of growth. Avascular growth, that which occurs when the tumor does not have its own vasculature, is the early phase of tumor growth that follows cell mutation (Byrne, 1999). During this stage, nutrients required for growth (such as glucose, oxygen (Folkman and Hochberg, 1973; Sutherland, 1988) or some other relevant nutrient) are supplied to the tumor via diffusion from distant blood vessels (Byrne, 1999). Aggressive growth, including the possibility of metastasis, occurs after an avascular tumor has developed its own vascular network and will not be considered in the model developed in this paper. Rather, we focus on the early stages of tumor growth in which the tumor is simply adjacent to nutrient supplying vasculature to allow for an investigation of the initial interactions between the immune system and the emerging tumor.

As a result of the external nutrient supply, avascular tumors often develop into approximately radially symmetric structures. Ferreira et al. (2002) have also shown that branch-like structures develop when tumor cells divide rapidly and consume nutrients required for mitosis much more rapidly than those required for survival. In radially symmetric tumors, the growing tumor is characterized by up to three layers—an outer rim of dividing cells with easy access to nutrients, an inner shell of non-dividing cells subjected to lower nutrient levels, and a central core of necrotic (dead) cells that die due to extremely low nutrient concentrations.

Tumor growth is often suppressed either naturally by the immune system of the host, or by outside intervention using chemotherapeutic and other drug treatments. The purpose of this study is to investigate the effects of the immune system on tumor growth. The effects of chemotherapeutic drugs have been investigated in similar work by Ferreira et al. (2003) and in the ODE models of de Pillis and Radunskaya (2001).

Fundamental to the immune system are the concepts of "self" and "non-self". The components of the immune system are located throughout the body and are charged with the responsibility of detecting and destroying entities which are foreign to the body (non-self), such as tumor cells, while simultaneously allowing entities that belong in the body (self) to remain and carry out their function (Paul, 2003; Perelson and Weisbuch, 1997). Tumor cells present different antigens from those of the cells from which they have mutated. These are the antigens that alert the immune system to the non-self nature of the tumor cell. When there is a failure in the immune system's surveillance of tumor cells, or when the immune suppression of tumor cells is insufficient, a tumor is able to grow and invade surrounding tissue (Kleinsmith et al., 2001).

While other components (such as macrophages) exist, in the model developed in this research we consider only two cell types to comprise the immune system. In particular, we model the natural killer (NK) cells of the innate immune system and the cytotoxic T lymphocytes

(CTLs) of the specific immune system. Essentially, it is in this way that the model developed herein is different from that of Ferreira et al. Both are hybrid PDE–CA models, but this work introduces the impact of the immune response on tumor development.

Natural killer cells are able to find and eliminate malignant cells while they undertake surveillance of the body for foreign components (Kleinsmith et al., 2001). Forming part of the innate immune system, natural killer cells are cytotoxic cells that are highly effective in lysing multiple (but specific) tumor cell lines (Paul, 2003). Unlike cells of the specific immune system, which are drawn to a location due to the presence of antigen, the natural killer cells are constantly present guarding the body from infection and disease.

On the other hand, CTLs are able either to lyse or to induce apoptosis in cells presenting *specific* antigens, such as tumor cells (Paul, 2003). Unlike NK cells, CTLs are only able to recognize a specific antigen or tumor cell line. It is known however, that these cells are able to destroy more than one tumor cell during their life cycle while a single natural killer cell generally kills very few (Kuznetsov, 1997). After destroying the target cell, the CTLs move on in search of other antigen presenting cells.

Using the modeling framework described in this paper, we also demonstrate lymphocyte infiltration of tumors. This is of particular interest given recent experimental research that suggests improved survival rates for patients with intratumoral immune cells (Zhang et al., 2003). Infiltration of T cells into the tumor mass can also lead to fibrosis and necrosis, and therefore tumor destruction and antitumor immunity (Schmollinger et al., 2003; Soiffer et al., 1998). Tumors reduced in size are then more amenable to treatment by traditional radiation methods. Numerical solutions produced using the model developed in this paper are in qualitative agreement with the experimental results demonstrated by Zhang et al. (2003), Schmollinger et al. (2003), and Soiffer et al. (1998).

In the following section, the above biological description will be translated into the mathematical model used to simulate tumor growth and the interaction of the tumor with the immune system.

3. Model formulation

In this model we consider the nutrient limited growth of an early stage tumor and the dynamic interplay between the immune system and the growing tumor. The model involves a combination of reaction–diffusion equations for the nutrient species and numerous rules of evolution for the cellular automaton description of the various cell types that comprise the tissue–tumor environment.

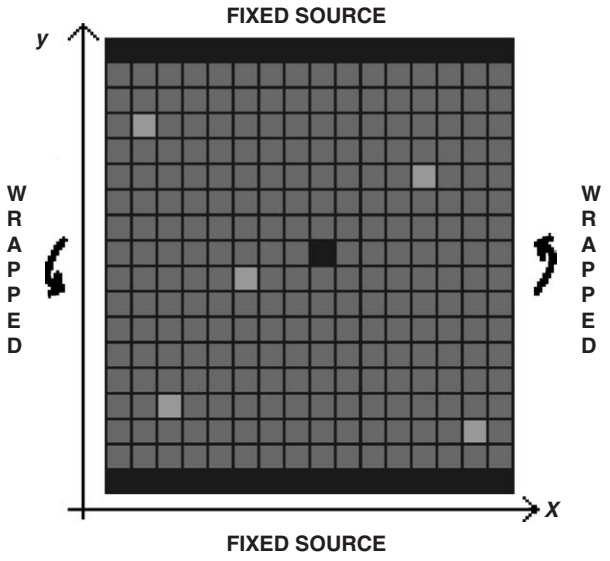

Fig. 1. Schematic of the cellular automata physical domain. The conditions imposed on the four boundaries are indicated. The solid bars (top and bottom) represent the capillaries while different cell types are shown filling the spaces in the grid.

We consider a tumor growing on a square domain $\Omega = [0, L] \times [0, L]$, where L is the length of each side of the domain. The spatial domain represents a two-dimensional patch of tissue that is supplied with nutrients by blood vessels that occupy the $y = 0$ and $y = L$ boundaries, as shown in Fig. 1. The remainder of the space is partitioned into a regular grid in which the various cell types reside, and through which the nutrient species diffuse. The grid is partitioned in such a way that each cellular automata grid element corresponds in size with the actual biological cells of interest (10–20 μm; Alarcon et al., 2003; Lin, 2004). While finer grids can be used for the nutrient PDE solver, sufficient accuracy was gained with the matching grids and this allowed for faster computation of solutions.

We simulate the temporal progression of the system using two main steps. First, the partial differential equations for the nutrient species are solved, then with dependence upon the new nutrient fields the cellular activities (such as motion and division) are carried out. Each temporal iteration therefore corresponds to the period of tumor cell division. That is, a period of approximately 0.5–10 days, depending on the cell type in question (Kirschner and Panetta, 1998; Riedel, 2004). The cellular automaton rules, along with a description of the reaction–diffusion equations are given below. For reference, the variables and parameters used in the model are listed along with descriptions in Table 1.

Table 1
Variables and model parameters used in the hybrid model

Variable	Description
$N(x,y,t)$	mitosis nutrient concentration
$M(x,y,t)$	survival nutrient concentration
H	host cell number
T	tumor cell number
I	total immune cell number
Parameter	**Description**
α	rate of consumption of nutrient by host and immune cells
λ_N	excess consumption factor of tumor over non-tumor cells of N nutrient
λ_M	excess consumption factor of tumor over non-tumor cells of M nutrient
P_{nec}	probability of tumor cell death due to necrosis
θ_{nec}	shape parameter for necrotic death probability curve
P_{imdth}	probability of tumor cell death due to the immune system
P_{div}	probability of tumor cell division
θ_{div}	shape parameter for cell division probability curve
P_{mig}	probability of tumor cell migration
θ_{mig}	shape parameter for migration probability curve
κ	number of possible tumor cell kills for a single CD8+ cell
I_0	background level of natural killer cells
P_{nk}	probability of the production of a new natural killer cell
P_L	probability of induction of a CTL due to CTL/TC interaction
θ_L	shape parameter for CTL induction probability curve
P_{LD}	probability of CTL death
θ_{LD}	shape parameter for CTL death probability curve

3.1. Reaction–diffusion equations

Reaction–diffusion equations have been widely used since the early models of (Greenspan, 1972) and Burton (1966) for the mathematical treatment of nutrient species, and many other chemical species, in tumor-growth models. In a similar manner, reaction–diffusion partial differential equations are also employed in this work to describe the distribution of two chemicals necessary for mitosis and cell survival.

As in the work of Ferreira et al. (2002, 2003), here we consider two nutrient species—the first nutrient being a necessary component of the cell division processes, while the second is essential for cellular survival. The nutrients diffuse throughout the tissue space, and as they do so they are consumed by the different cells that are resident in tissue.

The nutrient species are governed by the following equations:

$$\frac{\partial N}{\partial t} = D_N \nabla^2 N - k_1 HN - k_2 TN - k_3 IN, \tag{1}$$

$$\frac{\partial M}{\partial t} = D_M \nabla^2 M - k_4 HM - k_5 TM - k_6 IM, \tag{2}$$

where N and M represent the proliferation nutrient and survival nutrient, respectively. The cell species are identified by H for host cells (normal tissue), T for tumor cells, and I for immune cells. Also, D_N and D_M are the diffusion coefficients for the two nutrients, k_1, k_2 and k_3 are the rates of consumption of proliferation nutrient by host cells, tumor cells and immune cells, respectively, while k_4, k_5 and k_6 are the corresponding rates for the survival nutrient.

So as to maintain continuity of comparison with the work of Ferreira et al., upon which the above equations are based, we assume that the diffusion coefficients for both nutrients are equal. That is, $D_M = D_N = D$. Furthermore, we make similar assumptions for the consumption rates of the two chemicals by non-tumorous cells, and consider both normal tissue and immune cells to consume nutrients at the same rate such that $k_1 = k_4 = k_3 = k_6$. To model the increased nutrient consumption of tumor cells compared with that of normal cells, we further assume that the consumption rate of the tumor cells is a constant multiple of the host cell consumption rates. That is, $k_2 = \lambda_N k_1$ and $k_5 = \lambda_M k_1$, where $\lambda_N \geqslant 1$ and $\lambda_M \geqslant 1$ determine the excess consumption by the tumor cells of the two types of nutrient.

As mentioned above, we assume blood vessels pass through the area of interest and take for example, a pair of blood vessels residing along the boundaries $y = 0$ and $y = L$. Given that the blood vessel is the primary source of nutrient supply, the conditions at those boundaries for both reaction–diffusion equations take on the form $N(x,0) = N(x,L) = N_0$ and $M(x,0) = M(x,L) = M_0$. On the sides ($x = 0$ and $x = L$) we assume periodic boundary conditions.

To non-dimensionalise the reaction–diffusion equations, we assume the same variable transformations used by Ferreira et al. (2002), such that

$$\hat{t} = \frac{Dnt}{L^2}, \quad (\hat{x}, \hat{y}) = \left(\frac{nx}{L}, \frac{ny}{L}\right)$$
$$\hat{N} = \frac{N}{N_0}, \quad \hat{M} = \frac{M}{M_0}, \tag{3}$$

where variables under hats are dimensionless. With these transformations, Eqs. (1) and (2) in their non-dimensionalised form become

$$\frac{\partial N}{\partial t} = \nabla^2 N - \alpha^2 (H + I) N - \lambda_N \alpha^2 TN, \tag{4}$$

$$\frac{\partial M}{\partial t} = \nabla^2 M - \alpha^2 (H + I) M - \lambda_M \alpha^2 TM, \tag{5}$$

where $\alpha^2 = k_1 L^2 / Dn^2$ is the dimensionless rate of consumption of nutrient by host and immune cells and hats have been dropped for notational simplicity.

The change to non-dimensional variables also alters the source conditions on the $y = 0$ and $y = L$ boundaries. These become $N(x, 0) = N(x, n) = 1$ and $M(x, 0) = M(x, n) = 1$.

3.2. Cellular automata rules

While the chemical species are governed by deterministic reaction–diffusion equations, the evolution of the four cell species considered in this model proceeds according to a combination of probabilistic and direct rules. These are outlined below. As in Ferreira et al., we consider a simplification of the host cells being passive where, other than their consumption of nutrients, they allow tumor cells to freely divide and migrate.

3.2.1. Tumor cells

The tumor cells in this model undergo the processes of division, death, and movement. These processes depend upon nutrient levels, the presence of cells of the immune system, and crowding due to the presence of other tumor cells. At each time step, each cell is randomly assigned the option to divide, move or die, after which various conditions are checked to determine whether or not the action will be carried out. While it is possible that the time-scales of such processes may vary (between or within cell types), for generality we consider the time-scales to coincide with the time step of the numerical solution method. To effect the various changes to the tumor cell population, we impose the following cellular automata rules.

Due to their inherent mutations by which they avoid apoptosis, we do not consider natural death of tumor cells. We do however, consider two pathways to tumor cell death:

Death due to insufficient nutrient. If a cell is marked for death, the probability of cell death,

$$P_{nec} = \exp\left[-\left(\frac{M}{T\theta_{nec}}\right)^2\right] \tag{6}$$

is calculated to determine whether or not the action will be carried out. This probability term implies that the possibility of nutrient related death decreases as the ratio of nutrient M to the number of tumor cells T increases, with shape parameter θ_{nec}. This probability is of the same form as that used by Ferreira et al. (2002).

Death due to the immune system. When the cells of the immune system arrive in a close neighborhood of a tumor cell, the immune cells try to kill the tumor cell, with an intensity directly related to the strength of the local immune system. The probability of death in this case is given by

$$P_{imdth} = 1 - \exp\left[-\left(\sum_{j\in\eta} I_j\right)^2\right], \tag{7}$$

where the summation counts the total number of immune cells (both NK and CTLs), I, in the neighborhood, η, of the relevant tumor cell. Without further experimental information, we consider η to include the eight CA elements surrounding element j.

Tumor cells can undergo mitosis provided the local level of the mitosis nutrient, N, is sufficient.

Tumor cell division. If a cell is marked for division, the probability of cell division,

$$P_{div} = 1 - \exp\left[-\left(\frac{N}{T\theta_{div}}\right)^2\right] \tag{8}$$

is calculated to determine whether mitosis occurs. This term implies that the chance of division increases with the ratio of nutrient concentration to the number of tumor cells, with a shape parameter θ_{div}, and is of the form used by Ferreira et al. (2002).

The grid location upon which the daughter cell is placed depends upon the cells occupying the neighborhood of the mother cell. For example, a dividing cell with at least one host cell or necrotic space surrounding it will place its daughter cell randomly in one of those non-cancerous locations and either destroy the host cell or simply replace the necrotic material. On the other hand, if all elements around the dividing cell are filled with tumor cells, the daughter cell will be placed in the neighboring element containing the fewest tumor cells. This may be viewed as one approach to modeling tumor cell crowding.

Finally, tumor cells may also be chosen to move to a neighboring location on the cellular automata grid.

Tumor cell migration. Cells marked for migration do so with a probability given by

$$P_{mig} = 1 - \exp\left[-T\left(\frac{M}{\theta_{mig}}\right)^2\right], \tag{9}$$

such that the probability that the cell migrates increases with the tumor cell count of the current element. This is another way that cell crowding effects are accounted for in the model. This probability term, proposed by Ferreira et al. (2002), suggests that the likelihood of tumor cell movement increases with higher levels of the nutrient, M, possibly because nutrients allow the cell to proceed with migratory processes. It has also been considered that a cell may prefer to move away from areas of low nutrient concentration, and in this case the M in the probability term would appear in the denominator. Preliminary experiments with this model alteration have produced little qualitative difference to

solutions, however this will be investigated further in future research.

The grid location to which the migrating cell relocates again depends upon the cells that occupy its neighborhood. Migrating cells that have necrotic space or host cells in their immediate neighborhood will randomly move to one of these elements, replacing the original occupant as was the case for a daughter cell above. When all neighboring automaton elements are occupied by tumor cells, the migrating cell will move to the element with the fewest cancer cells—again in an attempt to move away from crowded areas of the tumor. While it has not been considered in this work, directed motion such as chemotaxis could be introduced to the model here by requiring the moving cell to move toward areas of higher nutrient levels.

While Eqs. (6), (8) and (9) are taken from Ferreira et al. (2002), and Eq. (7) is constructed from a similar point of view, different functional forms may indeed lead to slightly different results from the quantitative viewpoint, and with more experimental justification it will be possible to give more accurate probability functions. This is currently a topic of further research.

3.2.2. Immune cells

Two separate immune cell populations are considered here—the natural killer cells of the innate immune system, and cells of the specific immune response, represented by the CTLs.

Here we consider CTLs to be recruited to the tumor location from external sources when natural killer cells lyse tumor cells or when CTLs and tumor cells interact. Furthermore, the cells of the specific immune system are able to lyse tumor cells more than once (Kuznetsov, 1997). Hence, we assume that CTLs may kill a fixed number of tumor cells and use κ to represent this kill parameter.

Like the tumor cells, at each time step, immune cells that are near tumor cells are marked with the intent to carry out tumor cell lysis. On the other hand, those immune cells with no nearby tumor cells are randomly assigned to either die off or to attempt to migrate in search of tumor cells.

In this model we assume that natural killer cell numbers are roughly stable around some "normal" constant proportion, I_0, of the total number of cells in the domain. This is achieved by imposing an initial condition where $I_0 n^2$ NK cells are randomly placed over the domain of interest.

Natural killer cell production. In order to maintain the normal level of the natural killer cell population, we impose a form of birth on the evolution of the immune cell population. At each time step and for each CA grid element, a random number is generated and compared with the probability of natural killer cell production:

$$P_{nk} = I_0 - \frac{1}{n^2} \sum_{all\ CA} I. \tag{10}$$

If the random number is less than P_{nk} and the element is not currently occupied by a tumor cell, then a new natural killer cell will be placed in that element. This probability term, P_{nk}, effectively compares the current NK cell population in the domain of interest with the proportion that is expected in the normal situation. The effect of this strategy is that it allows NK cells to arrive in open spaces, possibly from below the domain of computation (in an attempt to incorporate at least some three-dimensionality in the model), but also in free spaces near the two blood vessels (at the top and bottom of domain).

Immune cell lysis of tumor cells. If an immune cell comes in contact with a tumor cell there is a probability that the immune cell will lyse the tumor cell. This rule corresponds to the rule for tumor cell death due to the immune system using Eq. (7).

- If the immune cell is a NK cell it is destroyed along with the tumor cell. Furthermore, the CA element is flagged for the induction of the specific immune system (through CTLs) at the next time step.
- If the immune cell is a CTL, the effectiveness of the cell is reduced—i.e., the number of remaining tumor cell kills, κ, is reduced by one.
- If the immune cell is a CTL, the surrounding CA elements are sampled for further CTL induction. For each neighboring free cell a random number is compared with

$$P_L = \exp\left[-\left(\frac{\theta_L}{\sum_{j\in\eta} T_j}\right)^2\right] \tag{11}$$

to determine whether or not further induction is initiated. In the expression for P_L the summation counts the number of tumor cells, T, in the neighborhood, η, of the relevant CA element, and θ_L is a parameter determining the shape of the probability curve. This lymphocyte recruitment facilitates the satellitosis where T cells have been observed surrounding tumor cells undergoing apoptosis (Soiffer et al., 1998). For completeness we note that for a neighboring tumor cell count of zero, P_L is defined to be zero also.

Immune cell death. CTLs are assumed to die by one of two means. Firstly, they become functionally useless (and therefore, not tracked by the program) when their cell kill value κ is reduced to zero. Secondly, the CTLs will die off or move away from the domain of interest if they no longer detect tumor cells in their neighborhood.

This death occurs with probability

$$P_{LD} = 1 - \exp\left[-\left(\frac{\theta_{LD}}{\sum_{j\in\eta} T_j}\right)^2\right], \quad (12)$$

where the summation counts all tumor cells in the neighborhood of the immune cell, θ_{LD} is a parameter determining the shape of the probability curve, and the probability of immune cell death is defined to be unity when there are no tumor cells nearby.

Immune cell migration. Immune cells that do not encounter a tumor cell at some point in time will continue to move randomly about the domain of interest.

- If there are tumor cells in neighboring CA elements, the immune cell will choose to attack one of these at random.
- If there are no tumor cells in neighboring CA elements, the immune cell will choose an element at random and move there.

We point out that while tumor antigenicity is not a direct component of these CA rules, antigenicity levels can be reflected in the model through the adjustment of the immune production and recruitment parameters, such as P_{nk}, P_L and θ_L.

Together, these cell rules and the partial differential equations describe the evolution of the tumor–immune system environment under consideration. To model an emerging tumor, the initial state of the system is taken as follows. The cellular automata grid houses a single mutated cancer cell along with the normal level, I_0, of natural killer immune cells. The remainder of space available to cells is occupied by non-tumorous host cells. As in other similar models (such as Alarcon et al., 2003; Ferreira et al., 2002, 2003; Patel et al., 2001), the nutrient species are assumed to be in a temporal steady-state distribution throughout the domain since the time-scale for nutrient diffusion is known to be much shorter than the time-scale for cell metabolism. The steady-state distribution being determined during the initial calculation of solutions to Eqs. (4) and (5).

4. Simulations and results

The model described in the previous section was implemented using MATLAB Release 13 (The Mathworks Inc, 2002). The dimensionless parameter values α, λ_M and λ_N and shape parameters for tumor cell behavior have been chosen to correspond with those used by Ferreira et al. (2002) for similar growth simulations. The shape parameters for the probabilities related to immune cell dynamics are unknown and will be investigated in this section.

The solution of the model proceeds via a sequence of steps and a summary of this algorithm is given below.

(1) Assign parameter values, discretise spatial domain and construct cell data structures with initial conditions.
(2) Solve steady-state PDEs with dependence upon initial cell conditions, to obtain initial chemical concentrations.
(3) Loop over the required number of time steps or until stop conditions are satisfied:
   (i) Assign random number to all CA locations for use in deciding actions of cells.
   (ii) For each cell location in turn, calculate probabilities of the relevant cell action (that is, tumor cell death, migration, division, or immune cell death, migration and induction), depending upon the random number assigned above and the calculated nutrient concentrations.
   (iii) Update the cell data structures according to the probabilities and random actions decided upon above.
   (iv) Recalculate the nutrient concentrations resulting from the changed cell conditions.
   (v) Stop if tumor reaches domain edge or is eradicated, otherwise proceed to next time step and return to (i).

The initial conditions are always taken to be a single, mutated cell, so we do not consider sensitivity to the initial tumor cell distribution. For all results shown and discussed in the text to follow, at least 20 simulations have been carried out in order to give a general result for the parameter sets reported. Unfortunately the simulations are computationally intensive and further investigation is therefore quite difficult.

4.1. Immune system-free growth

Our findings confirm those of Ferreira et al. (2002, 2003), in which simulations show that tumor morphology is dictated by relative consumption rates: lower consumption rates lead to more compact tumors while relatively higher consumption rates lead to a branchier morphology. Furthermore, we have found that it is indeed possible to simulate tumors that grow first exponentially, then linearly and finally reach a steady-zone of existence. Unlike the deterministic model of Greenspan (1972), the stochasticity of this model means that small fluctuations in the tumor size are still observed—however, it can be claimed that the tumor is in a zone of stability with regard to the total number of tumor cells in the mass.

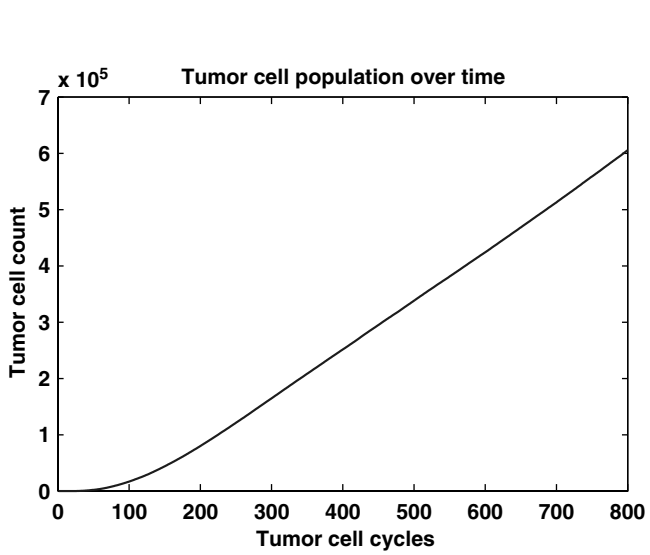

(a) Total tumor cell count over time.

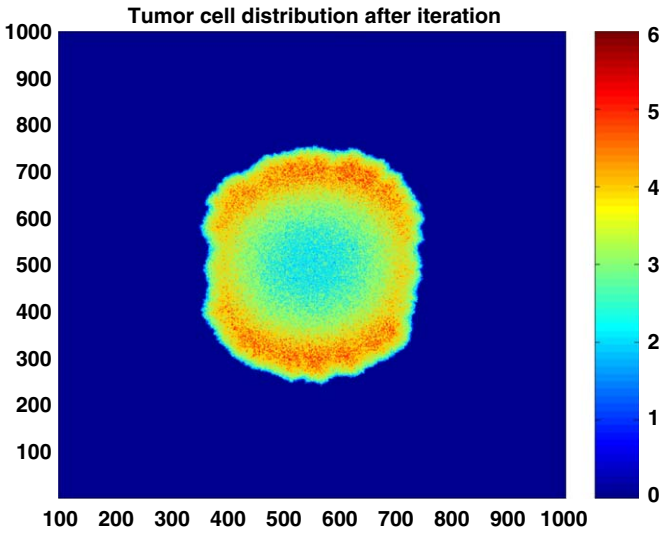

(b) Tumor cell distribution over the cellular automata grid.

Fig. 2. Compact tumor growth in the absence of immune system interaction. Parameter values are: domain size of 1000 elements $\approx 10-20$ mm, $t_{end} = 800$ cell division cycles, $\theta_{nec} = 0.03$, $\theta_{div} = 0.3$, $\theta_{mig} = 1000$, $\lambda_n = 50$, $\lambda_m = 25$, $\alpha = 1$, $I_0 = 0$. Note the beginning of a necrotic core in (b).

Fig. 2(a) shows the growth in the total number of tumor cells over time when the tumor is allowed to grow in the absence of any immune response. Note the initially exponential growth phase (iteration 0–200), before a phase of linear growth (iteration 200–800). These growth characteristics mimic the growth rates of multicell spheroids described experimentally by Folkman and Hochberg (1973) and mathematically by Greenspan (1972).

Fig. 2(b) displays the state of the system after 800 iterations. A roughly circular tumor with a radius of about 200 cells has developed in the center of the domain and is growing steadily toward the sources of the nutrient. Higher tumor cell densities are seen at the periphery of the tumor where it is surrounded by normal cells comprising the host tissue. In the center of the tumor a necrotic core is beginning to form with some necrotic material already appearing. The tumor shown is growing in a domain that is approximately 10–20 mm square, and over a time period of at least a year.

Using similar parameter values to those used by Ferreira et al. (2002), we reproduce the papillary tumor results from the same paper to provide a base point for a later consideration of the effects of the immune system. In relation to Fig. 2, the coefficients in the nutrient PDEs have been changed such that the rate of consumption by tumor cells of the mitosis nutrient is doubled, while the consumption rate of the survival nutrient is decreased by more than half. This allows the tumor cells to divide more rapidly in the direction of the nutrient supply and leads to the "branchy" nature of the resulting tumor shown in Fig. 3(b). Note also that a much larger domain size was used in Fig. 2 as when the domain sizes are smaller (as in Fig. 3), the compact tumor grows quickly to completely cover the domain shown and is less rounded in shape. We have used different domain sizes in order to best show the growth pattern of the two tumor types, prior to vascularization.

Fig. 3(a) shows the tumor cell count over time and it can be observed that the tumor is growing exponentially throughout the time considered without moving to a linear growth rate (as is seen in Fig. 2(a)). It appears that this is due to the shape of the tumor and the lower requirements of the tumor cells for survival nutrient. Unlike the spherical tumors for which the cell-dense periphery limits the diffusion of nutrients to the tumor center, the papillary tumor exhibits a fast expansion from its origin and does not form a cell-dense periphery. Nutrient diffusion throughout the domain is easier and more cells are provided with the nutrients to both survive and divide.

4.2. The effects of the immune system

In this section we investigate the changes to tumor growth when an immune system is introduced to the model. A review of relevant literature suggests that an appropriate range of values for I_0, the normal level of NK cells, is quite broad. For example Kaufmann (in Lin, 2004) suggests that the lymphocyte to tumor cell ratio can be anywhere from 5:1 to 1:100, depending on the tumor cell line. Cerwenker and Lanier (2001) state that up to 15% of lymphocytes are natural killer cells, and with lymphocytes comprising 10^{12} of the human body's 10^{13}–10^{14} cells (Encyclopædia Britannica, 2004), this gives a range for I_0 of between 0.1% and 1%.

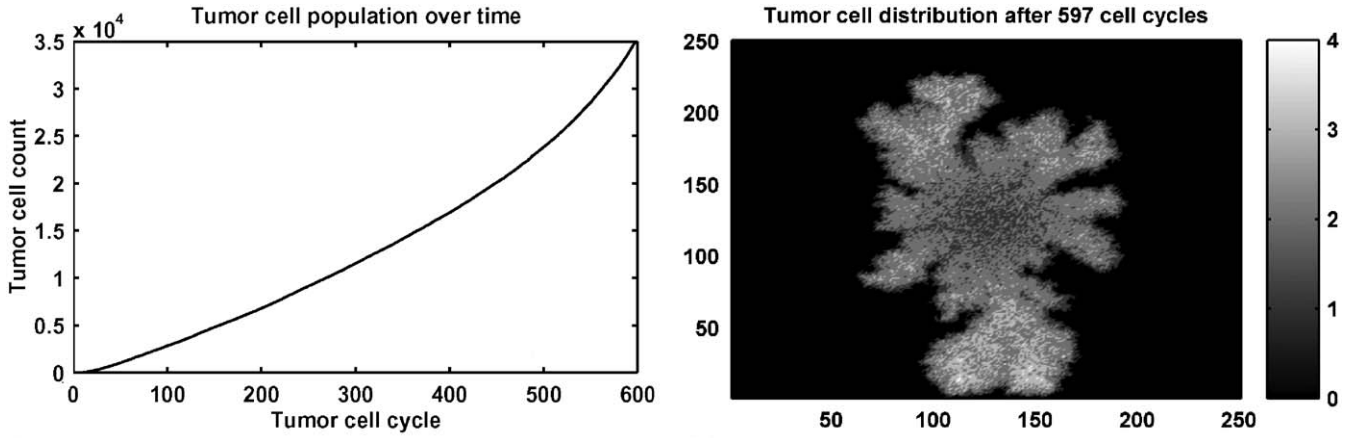

(a) Total tumor cell count over time. (b) Final tumor cell distribution over the cellular automata grid.

Fig. 3. An example of papillary tumor growth in the absence of immune system interaction. Parameter values are: domain size of 250 elements $\approx 2.5-4$ mm, $t_{end} = 597$ cell cycles, $\theta_{nec} = 0.03$, $\theta_{div} = 0.3$, $\theta_{mig} = 1000$, $\lambda_n = 100$, $\lambda_m = 10$, $\alpha = 2$, $I_0 = 0$.

Throughout the simulations to be presented we will employ a value of $I_0 = 0.01$ or 1%. Values above this were found to swamp the early development of tumors, and would therefore be indicative of an immune system of quite effective strength. For immune levels below 1%, little effect due to the immune system was evident, and while this would be indicative of a very weak immune system we do not investigate these possibilities due to their similarities to the immune system-free simulations of Section 4.1.

Fig. 4 show the effect on tumor (left figures) and total immune (right figures) cell populations, that is the sum of NK and CTL cell populations, due to changes in the CTL recruitment parameter θ_L. All figures were produced with the same parameters as Fig. 2 (except for the immune parameters) and show oscillatory population cell counts for both tumor and total immune cells. While these results apply directly to the simulations using compact-tumor parameters, qualitatively similar results were observed for simulations using the papillary-tumor parameters.

Figs. 4(a) and (b) show solutions for the lowest value of θ_L, when recruitment of CTLs following NK-induced tumor cell apoptosis is high, and very few oscillations are observed. The tumor grows exponentially to around 15 cells before immune recognition which decreases the tumor size. The tumor begins another growth stage at iteration 25, as it has undergone sufficient shrinkage to evade the immune cells present at that time. The tumor grows to 35 cells, before the immune system again detects it and fully eradicates the growth at iteration 42. While it appears in Fig. 4(b) that little has changed in the immune cell population, the important factor is the *location* of the immune cells. After detection of the tumor, the immune cells are attracted to the location of the tumor mass, thus aiding in its removal.

For $\theta_L = 5$, solutions are shown in Figs. 4(c) and (d). The tumor cell population is quite oscillatory and is almost reduced to zero on a number of occasions. However, over time the tumor cell population grows to a somewhat steady level, oscillating between 150 and 550 cells. A number of simulations carried out with this parameter set also exhibited this almost stable, oscillatory behavior. These results are similar to the purely temporal results of Kirschner and Panetta (1998), where oscillations were also observed in effector and tumor cell populations. Experimental evidence for such oscillatory behavior can also be found in works such as that due to Krikorian et al. (1980) regarding non-Hodgkin's lymphoma.

In Figs. 4(e) and (f) the tumor and total immune cell populations are shown for the case where CTL induction is low. In this example, the tumor cell population is only slightly oscillatory. Furthermore, the population grows exponentially (although at a slower rate than in Fig. 2) for the majority of the simulation. Near the end of the observed period of time, the tumor cell population begins to oscillate around 14,000 cells. In other simulations using this parameter set, the low recruitment of T cells leads to the tumor undergoing unstable, oscillatory growth where it appears to be growing without any bounds due to the immune system. While the stochastic nature of the model leads to difficulties in determining when the solution behaviors change, simulations indicated that tumor growth becomes unstable for values of the CTL recruitment parameter near $\theta_L = 5.5$.

Fig. 5 show the effect on tumor (left figures) and total immune (right figures) cell populations due to changes in the CTL death parameter θ_{LD}. All figures were produced with the same parameters as the compact tumor in Fig. 2 (except for the immune parameters) and again,

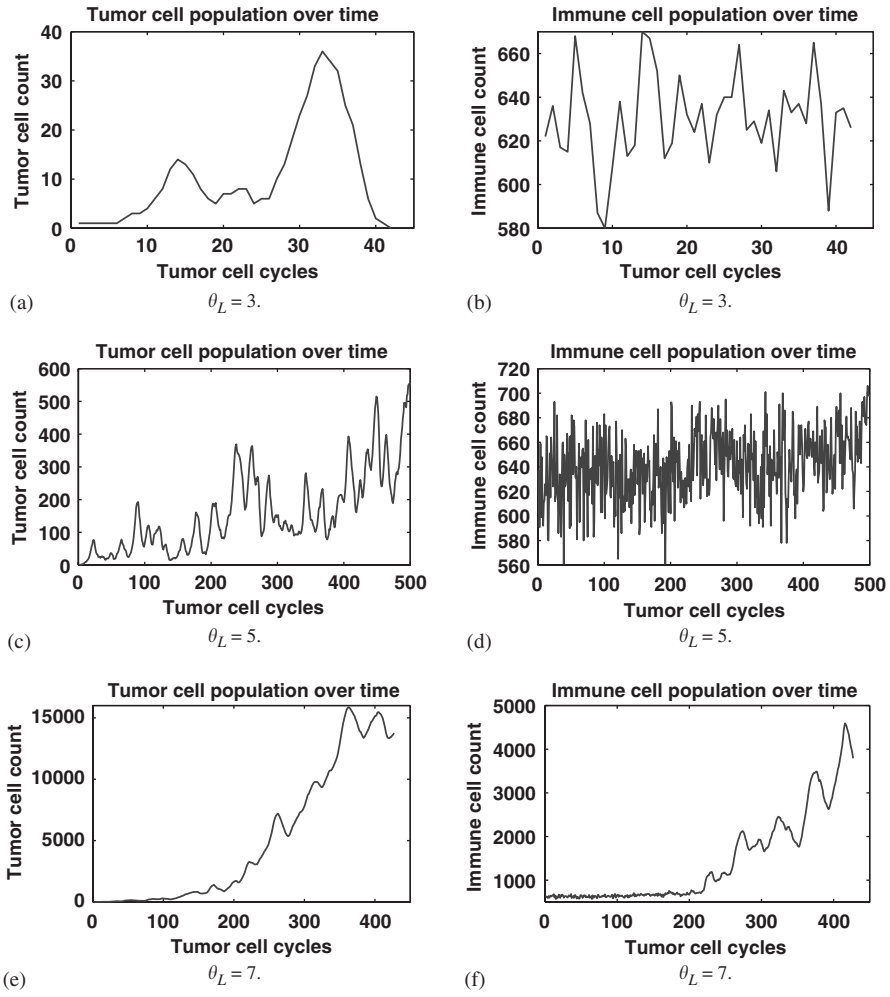

Fig. 4. The effect on tumor and total (NK + CTL) immune cell distributions in compact tumors over time due to changes in CTL recruitment rates (i.e. changes in θ_L). Parameter values are: domain size of 250 elements $\approx 2.5-4$ mm, $\theta_{nec} = 0.03$, $\theta_{div} = 0.3$, $\theta_{mig} = 1000$, $\lambda_n = 100$, $\lambda_m = 10$, $\alpha = 2$, $I_0 = 0.01$, $\theta_{LD} = 0.3$.

oscillatory population cell counts are observed for both tumor and the total population of immune cells. Note that qualitatively similar results were also observed for simulations using the papillary-tumor parameters, although the change from stable-oscillatory to unstable-oscillatory growth occurred at a slightly higher θ_{LD} value for the papillary tumors.

Figs. 5(a) and (b) show solutions for the lowest value of θ_{LD}, indicating lower probabilities of CTL death in regions of low tumor presence. The solution shows a tumor cell population with basically two oscillations before eradication. Note that after the first response by the immune system, a 50 cell tumor is reduced to only one cancerous cell. Exponential growth again occurs before a complete eradication of the tumor by the immune cells.

The second row of figures (Figs. 5(c) and (d)) show tumor and total immune cell populations over time for $\theta_{LD} = 0.5$. That is, a higher probability of CTL death when tumor cell levels are low. Again the tumor cell population oscillates, although about six times longer than the previous example and with tumor populations approximately six times greater in the largest oscillations. This tumor is however, eventually destroyed by the response of the immune system.

In the final pair of solution plots, Figs. 5(e) and (f), unstable oscillatory tumor growth is evident. Here the CTL death parameter is set to $\theta_{LD} = 0.7$, which is a substantially lower death probability than for the first pair of Fig. 5 where tumor destruction was quite fast. In this simulation, it appears that initially the tumor is in a phase of somewhat stable, oscillatory growth. However, near the end of the simulation (where the tumor reached the edge of the spatial domain), the tumor cell population appears to have broken out of this stable pattern and is growing in an unstable manner. Simulations indicated that tumor growth for compact-tumor simulations becomes unstable when the CTL death

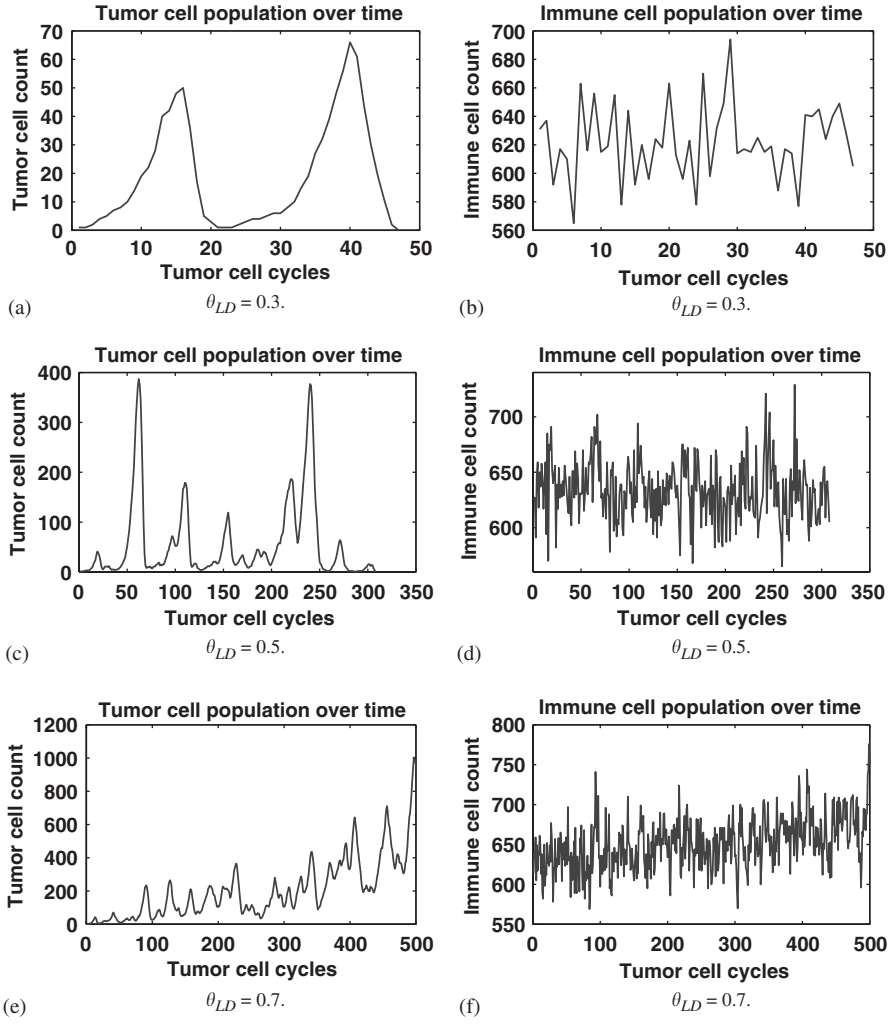

Fig. 5. The effect on tumor and total (NK + CTL) immune cell distributions in compact tumors over time due to changes in CTL death rates (i.e. changes in θ_{LD}). Parameter values are: domain size of 250 elements $\approx 2.5-4$ mm, $\theta_{nec} = 0.03$, $\theta_{div} = 0.3$, $\theta_{mig} = 1000$, $\lambda_n = 50$, $\lambda_m = 25$, $\alpha = 2$, $I_0 = 0.01$, $\theta_L = 3$.

parameter was set near $\theta_{LD} = 0.58$, while for papillary-tumor parameters the critical parameter value was approximately $\theta_{LD} = 0.63$.

4.3. Lymphocyte infiltration

In this section we present a particularly interesting application of the model which produces simulations that are qualitatively similar to the results of some recent experimental studies. Recent experimental studies have discussed the relationship between increased survival rates of cancer patients, tumor necrosis and fibrosis, and the presence of intratumoral T cells, or infiltrated T lymphocytes (Schmollinger et al., 2003; Soiffer et al., 1998; Zhang et al., 2003). The results shown in Fig. 6 simulate the infiltration of immune cells into a growing tumor. These are seen in the darker regions of Fig. 6(b) where tumor cell necrosis has occurred, and in the lighter regions of Fig. 6(d) where the immune cell numbers are highest. These solution plots are similar to experimental results shown by Schmollinger et al. (2003), Soiffer et al. (1998), and Zhang et al. (2003) where strings of immune cells are moving into the tumor, surrounding individual cells and causing tumor cell necrosis.

The simulation shown uses parameters for a compact tumor (in the absence of the immune system), low level CTL recruitment and low CTL death probability. Here we note that the tumor is able to continue to grow in size even though its structure is depleted in a random manner and necrotic regions are visible throughout the tumor. Essentially, the immune system is chasing the tumor but unable to successfully contain it due to the excessive proliferation of the tumor cells.

A number of experimental studies have produced similar patterns of tumor infiltration by immune cells as those found through solution of the mathematical model

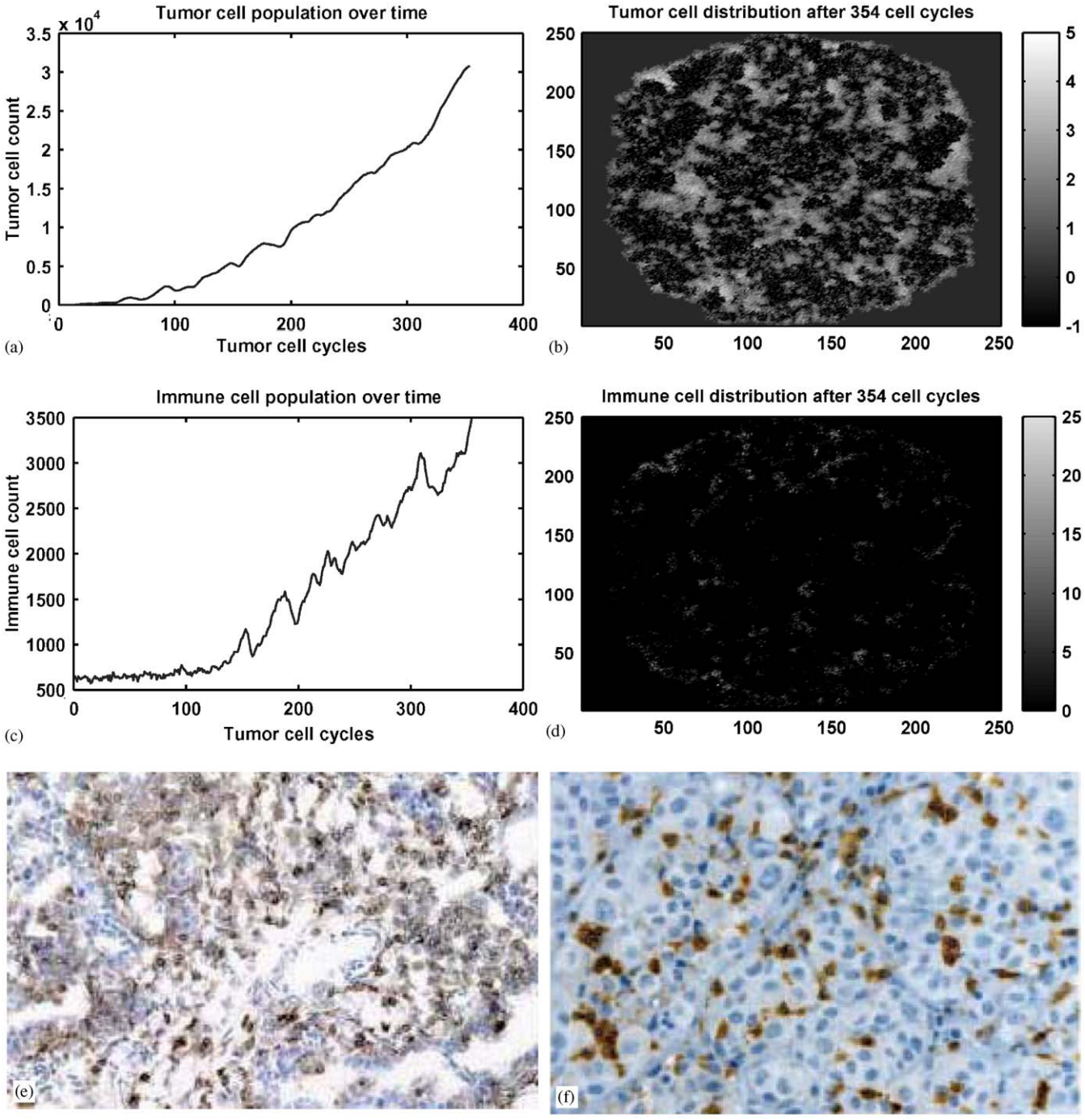

Fig. 6. Immune cell infiltration into a growing tumor. (a) and (b) show the tumor cell count over time and the final tumor cell distribution over the cellular automata grid, while the same outputs for total immune cells are shown in (c) and (d). Parameter values are: domain size of 250 elements $\approx 2.5-4$ mm, $t_{end} = 354$ cell division cycles, $\theta_{nec} = 0.03$, $\theta_{div} = 0.3$, $\theta_{mig} = 1000$, $\lambda_n = 50$, $\lambda_m = 25$, $\alpha = 1$, $I_0 = 1\%$, $\theta_L = 9$, $\theta_{LD} = 0.9$. Computations were halted when the tumor cells reached the edge of the computational domain. (e) and (f) show T cell infiltration in ovarian carcinoma (from Zhang et al. (2003) used with permission, copyright © Massachusetts Medical Society, 2003) and colon metastasis (from Schmollinger et al. (2003) used with permission, copyright © National Academy of Sciences, 2003), respectively.

developed in this paper (see for example, Schmollinger et al., 2003; Soiffer et al., 1998; Zhang et al., 2003). Shown in Fig. 6(e) are patterns of T cell infiltration in ovarian carcinoma (taken from Zhang et al. (2003)). Tumor cells (blue) have been extensively infiltrated by the immune cells (gray). In Fig. 6(f), a colon metastasis (blue cells) has been extensively infiltrated by CD8+ T cells (black) (taken from Schmollinger et al. (2003)). Small areas of tumor necrosis (white) can be seen in the region of the immune cells.

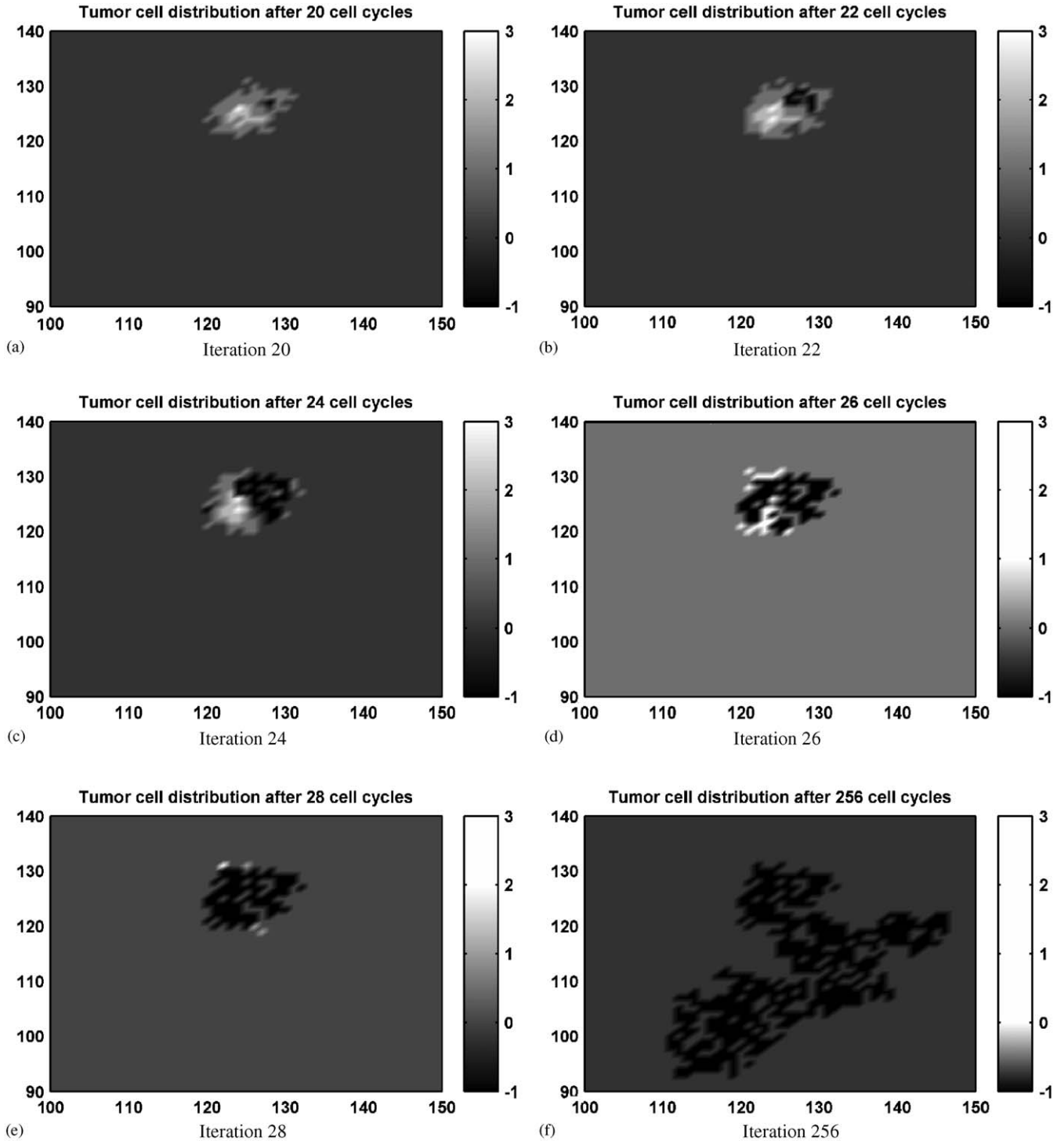

Fig. 7. Six time frames of immune cell infiltration into a growing tumor leading to tumor destruction. Heavy damage is inflicted early in the tumor growth process. Parameter values are: domain size of 250 elements $\approx 2.5-4$ mm, $t_{end} = 256$ cell division cycles, $\theta_{nec} = 0.03$, $\theta_{div} = 0.3$, $\theta_{mig} = 1000$, $\lambda_n = 50$, $\lambda_m = 25$, $\alpha = 1$, $I_0 = 1\%$, $\theta_L = 4$, $\theta_{LD} = 0.4$.

Fig. 7 show the infiltration of T cells into the growing tumor over time and the resulting tumor destruction. In this simulation, the greater T cell recruitment and lower death rate (compared with the parameters for Fig. 6) cause an early and strong immune response to the young tumor, as seen in Fig. 7(a)–(e). Over the remainder of the period of growth, up until total destruction at iteration 256, the tumor cell population undergoes oscillatory growth. The tumor cells grow away from the immune cells in an attempt to evade them, while the immune cells are constantly directed to surround and kill the tumor cells. Eventually the cell division of the

tumor cells is not sufficient to exceed the level of cell lysis by immune cells and the tumor is destroyed.

5. Conclusion

We have employed a moderately complex, hybrid cellular automata-partial differential equation model to describe interactions between a growing tumor and the immune system.

The model includes both the growth dynamics of tumors and the effects on tumor growth of the innate and specific immune systems. Each tumor cell is given the opportunity to move or divide, and is killed when the local survival nutrient levels are too low. The immune system is modeled by the inclusion of both natural killer cells and cytolytic T lymphocytes, both of which are able to lyse cancer cells. While NK cells can kill only one tumor cell, this initial detection of mutated cells leads to recruitment of specific immune cells (CTLs) that are able to lyse tumor cells many times. The probability of tumor cell lysis by immune cells is increased for strong local immune systems. A background level of NK cells is maintained over time to allow for the innate immune system's surveillance role. After lysing a tumor cell, T lymphocytes continue to roam the domain in search of further target cells, although they may move out of the domain of interest or die if the local tumor cell density is low.

In the absence of the immune system, the model is able to reproduce tumors of both compact-circular and papillary morphologies. These tumor shapes have direct dependence on the relative rates of consumption of the survival and mitosis nutrients by both tumor and host tissue cells. For circular tumors, the two-dimensional analogue of the spherical tumor, simulations show the presence of necrotic cores and outer bands of proliferating cells. These results correspond qualitatively with the experimental literature (such as Folkman and Hochberg, 1973).

Introducing the immune system to the model leads to various results depending on the choice of T lymphocyte recruitment and death parameters. For virtually all immune system parameter choices, the resulting solutions displayed oscillatory behavior for tumor and immune cell populations in a similar manner to ODE models of tumor–immune system interactions. Depending on the strength of T cell recruitment and the T cell death parameter, the tumor grew with stable or unstable oscillations and in some cases the tumor was destroyed completely. Due to the probabilistic nature of the model, it is difficult to determine exact parameter values at which the tumor growth becomes unstable. For the parameter sets shown in Figs. 4 and 5, approximate values determined through repeated simulation are given in Section 4.2.

The varying parameter value sets correspond to strong immune systems of healthy individuals, capable of early tumor detection and destruction, and weaker immune systems of individuals for whom tumors grow easily or are at least able to grow to the point of metastasis and hence migrate throughout the body. Furthermore, simulations indicate that (as would be expected) increasing lymphocyte recruitment and increasing the cytolytic ability of lymphocytes leads to greater reductions in tumor size. Such lymphocyte recruitment could be effected through vaccinations with irradiated tumor cells, engineered to secrete chemoattractants such as those used in the work of Schmollinger et al. (2003).

Finally, we used the model to demonstrate T cell infiltration into tumor growths. Experimental literature has shown that greater survival rates are observed in patients with lymphocyte infiltrates in tumors. Using the model proposed in this paper we have determined the parameter regimes in which infiltration is effective in tumor destruction. It is the subject of another study of the authors' to model the effects of injected T cells and T cell infiltration on pre-grown tumors.

There is clinical evidence that immune cells play an important role in the control of certain malignancies, a fact that is exploited in the development of immunotherapies for cancers (see, for example Blattman and Greeberg, 2004; Couzin, 2002; Donnelly, 2003; Pardoll, 1998; Rosenberg et al., 2004; Wheeler et al., 2004). Of the large array of immunotherapy types available, one that might be readily included in this model structure is the direct injection of tumor infiltrating lymphocytes (see, for example, Dudley et al., 2002). In future studies, the model employed here will be extended to consider the effects of immunotherapy on the interactions between the immune system and growing tumors.

In summary, while the cellular automata rules proposed in this model are not definitive choices, we have successfully proposed a framework for including the immune system in a hybrid CA–PDE model of tumor growth. The resulting solutions are in qualitative agreement with both the experimental and theoretical literature, including both PDE models of tumor growth and ODE models of tumor–immune system interactions. It has been shown that the simple description proposed here regarding immune and tumor cell interactions, and the use of hybrid CA–PDE models, have the potential to produce the behavior observed in some experiments. What needs to follow this work is an exploration of the robustness of the model to different functional forms, as well as the derivation of actual parameters and accurate functional forms from experimentalists. With the introduction of such elements it will be possible to judge if this is actually how the observed phenomena occur and if this modelling strategy is appropriate.

Acknowledgements

D.G. Mallet thanks Harvey Mudd College for a Postdoctoral Fellowship during which a proportion of this work was completed.

References

Adam, J.A., Bellomo, N., 1997. A Survey of Models for Tumor–immune System Dynamics. Birkhauser, Basel.

Alarcon, T., Byrne, H.M., Maini, P.K., 2003. A cellular automaton model for tumour growth in inhomogeneous environment. J. Theor. Biol. 225, 257–274.

Anderson, A.R.A., Chaplain, M.A.J., 1998. Continuous and discrete mathematical models of tumor induced angiogenesis. Bull. Math. Biol. 60, 877–900.

Araujo, R.P., McElwain, D.L.S., 2004. A history of the study of solid tumour growth: the contribution of mathematical modelling. Bull. Math. Biol. 66, 1039–1091.

Arciero, J.C., Jackson, T.L., Kirschner, D.E., 2004. A mathematical model of tumor–immune evasion and siRNA treatment. Discrete Continuous Dynamical Systems—Ser. B 4 (1), 39–58.

Bard Ermentrout, G., Edelstein-Keshet, L., 1993. Cellular automata approaches to biological modeling. J. Theor. Biol. 160, 97–133.

Bellomo, N., Preziosi, N., 2000. Modelling and mathematical problems related to tumor evolution and its interaction with the immune system. Math. Comput. Modelling 32, 413–452.

Bellomo, N., Firmani, B., Guerri, L., 1999. Bifurcation analysis for a nonlinear system of integro-differential equations modelling tumor–immune cells competition. Appl. Math. Lett. 12, 39–44.

Blattman, J.N., Greeberg, P.D., 2004. Cancer immunotherapy: a treatment for the masses. Science 205, 200–205.

Burden, T., Ernstberger, J., Renee Fister, K., 2004. Optimal control applied to immunotherapy. Discrete Continuous Dynamical Systems—Ser. B 4 (1), 135–146.

Burton, A.C., 1966. Rate of growth of solid tumours as a problem of diffusion. Growth 30, 159–176.

Byrne, H.M., 1997. The importance of intercellular adhesion in the development of carcinomas. IMA J. Math. Appl. Med. Biol. 305323, 14.

Byrne, H.M., 1999. Using mathematics to study solid tumour growth. In: Proceedings of the Ninth General Meetings of European Women in Mathematics, pp. 81–107.

Byrne, H.M., Chaplain, M.A.J., 1995. Growth of nonnecrotic tumours in the presence and absence of inhibitors. Math. Biosci. 151181, 130.

Byrne, H.M., Chaplain, M.A.J., 1996. Modelling the role of cell–cell adhesion in the growth and development of carcinomas. Math. Comput. Modell. 24 (12), 1–17.

Byrne, H.M., Chaplain, M.A.J., 1997. Free boundary value problems associated with the growth and development of multicellular spheroids. Eur. J. Appl. Math. 8, 639–658.

Callewaert, D.M., Meyers, P., Hiernaux, J., Radcliff, G., 1988. Kinetics of cellular cytotoxicity mediated by cloned cytotoxic T lymphocytes. Immunobiology 178, 203–214.

Cerwenker, A., Lanier, L.L., 2001. Natural killer cells, viruses and cancer. Nat. Rev. Immunol. October, 41–48.

Couzin, J., 2002. Select T cells, given space, shrink tumors. Science 297, 1973.

Donnelly, J., 2003. Cancer vaccine targets leukemia. Nat. Med. 9 (11), 1354–1356.

Dormann, S., Deutsch, A., 2002. Modeling of self-organized avascular tumor growth with a hybrid cellular automaton. In: Silico Biol. 2, 0035.

Drasdo, D., Loeffler, M., 2001. Individual-based models on growth and folding in one-layered tissues: intestinal crypts and early development. Nonlinear Anal. 47, 245–256.

Dudley, M.E., Wunderlich, J.R., et al., 2002. Cancer regression and autoimmunity in patients after clonal repopulation with antitumor lymphocytes. Science 298 (5594), 850–854.

Encyclopædia Britannica. 2004. Cell. Encyclopædia Britannica Online. [Online] http://search.eb.com/eb/article?tocId=9106125.

Ferreira Jr., S.C., Martins, M.L., Vilela, M.J., 2002. Reaction–diffusion model for the growth of avascular tumor. Phys. Rev. E 65, 021907.

Ferreira Jr., S.C., Martins, M.L., Vilela, M.J., 2003. Morphology transitions induced by chemotherapy in carcinomas in situ. Phys. Rev. E 67, 051914.

Folkman, J., Hochberg, M., 1973. Self-regulation of growth in three dimensions. J. Exp. Med. 138, 745–753.

Franks, S.J., Byrne, H.M., King, J.R., Underwood, J.C.E., Lewis, C.E., 2003. Modelling the early growth of ductal carcinoma in situ. J. Math. Biol. 47, 424–452.

Franks, S.J., Byrne, H.M., Mudhar, H., Underwood, J.C.E., Lewis, C.E., 2003. Modelling the growth of comedo ductal carcinoma in situ. Math. Med. Biol. 20, 277–308.

Franks, S.J., Byrne, H.M., Underwood, J.C.E., Lewis, C.E., 2005. Biological inferences from a mathematical model of comedo ductal carcinoma in situ of the breast. J. Theor. Biol. 232 (4), 523–543.

Galach, M., 2003. Dynamics of the tumor–immune system competition—the effect of time delay. Int. J. Appl. Math. Comput. Sci. 13 (3), 395–406.

Galle, J., Loeffler, M., Drasdo, D. Modeling the effect of deregulated proliferation and apoptosis on the growth dynamics of epithelial cell populations in vitro. Biophys. J. 88 (1), 62–75.

Gatenby, R.A., Gawlinski, E.T., 1996. A reaction–diffusion model of cancer invasion. Cancer Res. 56, 5745–5753.

Greenspan, H.P., 1972. Models for the growth of a solid tumor by diffusion. Stud. Appl. Math. 51, 317–338.

Kansal, A.R., Torquato, S., Harsh IV, G.R., Chiocca, E.A., Deisboeck, T.S., 2000. Simulated brain tumor growth dynamics using a three dimensional cellular automaton. J. Theor. Biol. 203, 367–382.

Kirschner, D., Panetta, J.C., 1998. Modeling immunotherapy of the tumor–immune interaction. J. Math. Biol. 37, 235–252.

Kleinsmith, L.J., Kerrigan, D., Spangler, S., 2001. National cancer institute: Science behind the news—understanding cancer. [Online] http://press2.nci.nih.gov/sciencebehind/cancer/cancer01.htm

Krikorian, J.G., Portlock, C.S., Cooney, D.P., Rosenberg, S.A., 1980. Spontaneous regression of non-Hodgkin's lymphoma: a report of nine cases. Cancer 46, 2093–2099.

Kuznetsov, V.A., 1997. Basic models of tumor–immune system interactions—identification, analysis and predictions. In: Adam, J.A., Bellomo, N. (Eds.), A Survey of Models for Tumor–immune System Dynamics. Birkhauser, Basel.

Kuznetsov, V., Knott, G., 2001. Modelling tumor regrowth and immunotherapy. Math. Comput. Modell. 33 (12/13), 1275–1287.

Lin, A., 2004. A model of tumor and lymphocyte interactions. Discrete Continuous Dynam. Systems—Ser. B 4 (1), 241–266.

Mallet, D.G., 2004. Mathematical modeling of the role of haptotaxis in tumour growth and invasion. Ph.D. Thesis, Queensland University of Technology, Brisbane, Australia.

The Mathworks, Inc., 2002. MATLAB Release 13. Natick, MA.

Matzavinos, A., Chaplain, M.A.J., 2004. Mathematical modelling of the spatio-temporal response of cytotoxic T-lymphocytes to a solid tumour. Math. Med. Biol. 21, 134.

McDougal, S.R., Anderson, A.R.A., Chaplain, M.A.J., Sheraratt, J.A., 2002. Mathematical modelling of flow through vascular networks: implication for tumour-induced angiogenesis and chemotherapy strategies. Bull. Math. Biol. 64, 673702.

Merrill, S.J., 1982. Foundations of the use of enzyme kinetic analogy in cell-mediated cytotoxicity. Math. Biosci. 62, 219–236.

Owen, M.R., Sherratt, J.A., 1997. Pattern formation and spatiotemporal irregularity in a model for macrophage–tumour interactions. J. Theor. Biol. 189 (1), 63–80.

Owen, M.R., Sherratt, J.A., 1998. Modelling the macrophage invasion of tumours: effects on growth and composition. IMA J. Math. Appl. Med. Biol. 15, 165–185.

Owen, M.R., Sherratt, J.A., 1999. Mathematical modelling of macrophage dynamics in tumours. Math. Models Methods Appl. Sci. 9 (4), 513–539.

Owen, M.R., Byrne, H.M., Lewis, C.E., 2004. Mathematical modelling of the use of macrophages as vehicles for drug delivery to hypoxic tumour sites. J. Theor. Biol. 226 (4), 377–391.

Pardoll, D.M., 1998. Cancer vaccines. Nat. Med. Vaccine 4 (5(Suppl.)), 525–531.

Patel, A.A., Gawlinski, E.T., Lemiueux, S.K., Gatenby, R.A., 2001. A cellular automaton model of early tumor growth and invasion: the effects of native tissue vascularity and increased anaerobic tumor metabolism. J. Theor. Biol. 213, 315–331.

Paul, W.E., 2003. Fundamental Immunology, fifth ed. Lippincott, Williams & Wilkins Publishers, Philadelphia, PA.

Perelson, A.S., Mackean, C.A., 1984. Kinetics of cell-mediated cytotoxicity: stochastic and deterministic multistage models. J. Math. Bio. 170, 161–194.

Perelson, A.S., Weisbuch, G., 1997. Immunology for physicists. Rev. Mod. Phys. 69 (4), 1219–1267.

Pettet, G.J., Please, C.P., Tindall, M.J., McElwain, D.L.S., 2001. The migration of cells in multicell tumor spheroids. Bull. Math. Biol. 63, 231–257.

de Pillis, L., Radunskaya, A., 2001. A mathematical tumor model with immune resistance and drug therapy: an optimal control approach. J. Theor. Med. 3, 79–100.

de Pillis, L.G., Radunskaya, A., 2003a. A mathematical model of immune response to tumor invasion. In: Bathe, K.J. (Ed.), Proceedings of the Second MIT Conference on Computational Fluid and Solid Mechanics, Computational Fluid and Solid Mechanics.

de Pillis, L.G., Radunskaya, A., 2003b. The dynamics of an optimally controlled tumor model: a case study. Math. Comput. Modell. 37, 1221–1244.

Please, C.P., Pettet, G.J., McElwain, D.L.S., 1999. Avascular tumour dynamics and necrosis. Math. Models Methods Appl. Sci. 9, 569–580.

Preziosi, L. (Ed.), 2003. Cancer Modelling and Simulation. Taylor & Francis Ltd., Chapman & Hall/CRC, London, Boca Raton, FL.

Riedel, H., 2004. Models for tumour growth and differentiations. In: Alison, M.R. (Ed.), The Cancer Handbook. Wiley, New York.

Rosenberg, S.A., Yang, J.C., Robbins, P.F., Wunderlich, J.R., Hwu, P., Sherry, R.M., et al., 2003. Cell transfer therapy for cancer: lessons from sequential treatments of a patient with metastatic melanoma. J. Immunother. 26 (5), 385–393.

Rosenberg, S.A., Yang, J.C., Restifo, N.P., 2004. Cancer immunotherapy: moving beyond current vaccines. Nat. Med. 10 (9), 909–915.

Schmollinger, J.C., Vonderhelde, R.H., Hoar, K.M., et al., 2003. Melanoma inhibitor of apoptosis protein (ML-IAP) is a target for immune-mediated tumor destruction. Proc. Natl Acad. Sci. USA 100 (6), 3398–3403.

Seiden, P.E., Celada, F., 1992. A model for simulating cognate recognition and response in the immune system. J. Theor. Biol. 158 (3), 328–357.

Smallbone, K., Gavaghan, D.J., et al., 2005. The role of acidity in solid tumour growth and invasion. J. Theor. Biol. 235 (4), 476–485.

Soiffer, R., Lynch, T., Mihm, M., et al., 1998. Vaccination with irradiated autologous melanoma cells engineered to secrete human granulocyte macrophage colony-stimulating factor generates potent antitumor immunity in patients with metastatic melanoma. Proc. Natl Acad. Sci. USA 95, 13,141–13,146.

Sutherland, R.M., 1988. Cell and environment interactions in tumor microregions: the multicell spheroid model. Science 240, 177–184.

Takayanagi, T., Ohuchi, A., 2001. A mathematical analysis of the interactions between immunogenic tumor cells and cytotoxic T lymphocytes. Microbiol. Immunol. 45 (1), 709–715.

Ward, J.P., King, J.R., 1997. Mathematical modelling of avascular-tumour growth. IMA J. Math. Appl. Med. Biol. 14, 3969.

Ward, J.P., King, J.R., 1999. Mathematical modelling of avascular-tumour growth—II. Modelling growth saturation. IMA J. Math. Appl. Med. Biol. 16, 171211.

Weinberg, R.A., 1996. How cancer arises. Sci. Am. 275 (3), 62.

Wheeler, C.J., Asha, D., et al., 2004. Clinical responsiveness of glioblastoma multiforme to chemotherapy after vaccination. Clin. Cancer Res. 10, 5316–5326.

Xu, Y., 2004. A free boundary problem model of ductal carcinoma in situ. Discrete Continuous Dynam. B 4 (1), 337–348.

Zhang, L., Conejo-Garcia, J.R., Katsaros, D., et al., 2003. Intratumoral T cells, recurrence, and survival in epithelial ovarian cancer. N. Eng. J. Med. 348 (3), 203–213.